

Impacts of Temperature on Airborne Particles in A Hospital Operating Room

Open
Access

Nazri Kamsah¹, Haslinda Mohamed Kamar^{1,*}, Muhammad Idrus Alhamid², Wong Keng Yinn¹

¹ Faculty of Mechanical Engineering, Universiti Teknologi Malaysia, 81310, UTM Johor Bahru, Johor, Malaysia

² Departemen Teknik Mesin, Fakultas Teknik, Universitas Indonesia, Kampus Baru – UI, Depok, 16424, Indonesia

ARTICLE INFO

Article history:

Received 23 February 2018

Received in revised form 15 March 2018

Accepted 6 April 2018

Available online 15 April 2018

Keywords:

Operating room, inlet air diffuser,
airborne particle, computational fluid
dynamics

ABSTRACT

A proper ventilation system is necessary for isolating and reducing airborne particles in a hospital operating room. Most healthcare uses a downward unidirectional (laminar) flow in the area of the operating table to give a sterile environment to the patient. However, the unidirectional downward airflow can easily be deviated due to a buoyancy force induced by heated surfaces such as a person's and medical lamp's surfaces. Therefore, the goal of this study is to investigate the effects of lamps and human body surface temperatures on particles distribution in the vicinity of the operating table inside an operating room. A simplified computational fluid dynamics (CFD) model of the operating room was developed using commercial software. An RNG k-epsilon turbulent flow model was used to simulate the airflow while a discrete phase model (DPM) was used to simulate the movement of the airborne particle of size 5 μm . Results of CFD simulations show that when the surgical lamp and staff surface temperatures were prescribed at 45°C and 37°C, respectively, a more significant amount of particles appear to be on the floor of the adjacent area of the operating table head section. On average, the particle concentration in the vicinity of the operating table increases by 16%.

Copyright © 2018 PENERBIT AKADEMIA BARU - All rights reserved

1. Introduction

Hospital operating room (OR) is a facility inside a hospital where surgical operations are carried out in a hygienic environment. The environment should hold a free pathological microorganism atmosphere, and it depends on the quality of air [21]. The air quality inside the operating room is affected by various types of chemicals such as waste anaesthetic, sterilizing substance and airborne particles. Usually, these chemicals and particles are referred as contaminants, and most of them are infectious to the patient and medical staffs. Through a proper distribution of ultraclean air, infectious particles can be isolated efficiently and diluted, and surgical site infection (SSI) rate could be controlled. An SSI is defined as any disease that follows an operative procedure and occurs at or

* Corresponding author.

E-mail address: haslinda@mail.fkm.utm.my (Haslinda Mohamed Kamar)

near the surgical incision within 30 days of the process [7, 10]. SSIs are ranked third amongst the most common Healthcare-Associated Infections (HAI). Nearly 13 - 17% [1-2] and 10 - 40% [22] of the total HAI cases reported in Europe and the US, respectively, are associated with SSI. Singh *et al.* [22] discovered that in over 27 million operations performed annually in the US, approximately 300,000 cases were caused by SSI, of which 8,000 ended up in fatalities. SSIs also contribute to additional treatment costs and prolong hospital stays. Extra costs of 3 to 29 thousand US dollars has been wasted on the hospital charges [9].

SSI is originated from microbial contamination of the air, and it depends on the type of surgery, and the behaviour of staff in the operating room [2, 3, 13]. Various types of microorganisms such as *Staphylococcus aureus*, *Sphingomonas paucimobilis*, *Pseudomonas aeruginosa*, *Stenotrophomonas maltophilia*, *Clostridium difficile*, *Legionella* spp. and *Pseudomonas aeruginosa* commonly exist in healthcare facilities. However, *Staphylococcus aureus* and Coagulase-negative staphylococcus (CoNS) are the main bacterial species found in the operating room, and they are the most common cause of SSI [11, 17]. SSI cannot be treated by ordinarily used antibiotics due to the increasing resistance of *Staphylococcus aureus* to conventional drugs, in which it is known as Methicillin-resistant *Staphylococcus aureus* (MRSA). MRSA fits to survive under dry conditions for a more extended period, especially in a less cleaned area [16]. Several studies suggested that the microbial level in operating rooms can be evaluated by assessing the number of particulate matters (PMs). The airborne particles with an aerodynamic diameter ranging from 5 μm to 10 μm are widely considered as the bacteria-carrying particles [8, 15].

To provide proper distribution of ultraclean air inside an OR requires an exclusive ventilation system that capable of producing a free particle sediments environment. To fulfil this requirement, the ventilation system must perform as a dual-functioning machine that could filter the unwanted residues and remove the existing particles to the adjacent area. The direction of the airflow and the rate of air-change (ACH) in the OR are the main factors in determining the amount of airborne particle settlement [12]. Most of operating rooms use laminar airflow (LAF) air-supply systems which equipped with a high-efficiency particulate air (HEPA) filters or ultra-low penetration air (ULPA) filters. The HEPA filters are designed to filter 99.97% of particles of a diameter size above 0.3 μm , and the ULPA filters are for filtering 99.999% of particles with 0.12- μm diameter size. Operating rooms in many developed countries use the ultraclean ventilation systems with the ULPA filters because they are capable of supplying clean air and provide excellent comfort conditions to the medical staffs and patient [4, 17].

However, in Malaysia, due to high construction and maintenance costs of the latter system, only the LAF air-supply systems with the HEPA filters are widely used. The LAF provides unidirectional airflow ventilation in the OR where the air supply diffuser is located at the ceiling directly above the operation area, with the low-level exhaust outlets at the room edge. Such the unidirectional laminar flow pattern is achievable with an air velocity at 0.46 m/s or below [5]. However, sufficient amount of clean air with such magnitude of air velocity does not assure the LAF system to provide the desired unidirectional airflow pattern. Obstacles found along the airflow path such as a surgical lamp and person could also affect the airflow streamline. The effects could be remarkable if these barriers are also dissipating heat and cause a rise in their surface temperatures. The hot surface objects could form a buoyancy force due to density difference in the adjacent air. The buoyance-driven airflow around the human body and lamps capable of deviating the airflow streamline and increasing bacteria-carrying particles toward the surgical wound [5].

Therefore, in this study, a steady-state numerical analysis was carried out to investigate the effects of surface temperatures of surgical lamps and medical staffs on particles distribution inside an operating room. The OR was equipped with a LAF system, and the analysis was concentrated in

the operation area which is in the vicinity of the operating table. Particles with the size of 5 μm diameter were assumed to discharge from exposed faces of the surgical staffs at a given mass flow rate. A simplified model of the operating room was developed using Computational Fluid Dynamics (CFD) software. An RNG k-epsilon turbulent model was employed to simulate the airflow while a discrete phase model (DPM) was used to simulate the transport of the particles.

2. Methodology

2.1 Simulations of Air Flow and Particles

A simplified three-dimensional CFD model of the operating room was developed based on the literature. The operating room was modelled with a vertical air supply system and four horizontal outlet grilles. The model consists of an operating table, an air inlet diffuser, four air exhaust grilles, four medical staffs and two surgical lamps as shown in Figure 1. The air inlet diffuser was placed at the ceiling of the operating room, directly above the operating table. Figure 2 illustrates the dimensions of the operating room CFD model.

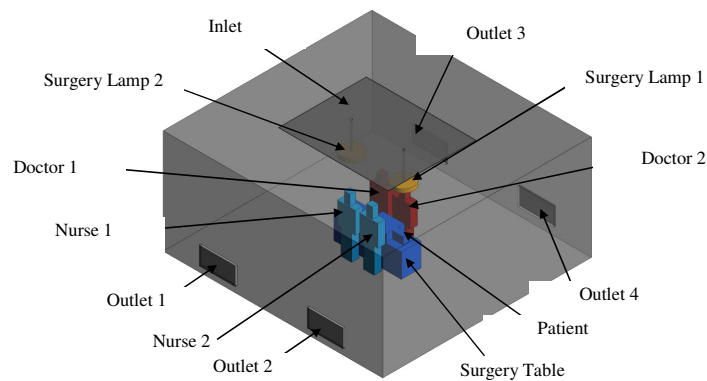


Fig. 1. Features of operating room CFD model

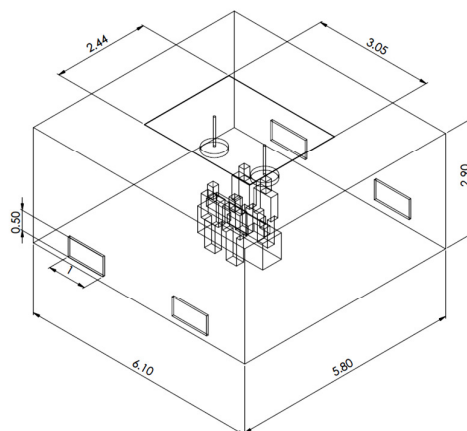


Fig. 2. Dimension of CFD model of the operating room (all dimensions are in meter)

The dimensions of the staffs, operating table and surgical lamps are given in Table 1.

Table 1

Dimensions of the medical staff, operating table and surgical lamp

Model	Dimensions
	(Length (m) × Width (m) × Height (m))
Medical staff	
- Body	0.3 × 0.2 × 0.6
- Head	0.16 × 0.16 × 0.30
- Hand	0.1 × 0.2 × 0.6
- Leg	0.3 × 0.2 × 0.7
Patient	
- Body	0.6 × 0.3 × 0.2
- Head	0.30 × 0.16 × 0.16
- Hand	0.6 × 0.1 × 0.2
- Leg	0.7 × 0.3 × 0.2
Surgical lamp	0.58 × 0.01 × 0.58
Operating table	1.88 × 0.54 × 0.66

2.2 Meshing of the Computational Domain

The CFD computational domain was meshed using an unstructured grid of tetrahedral elements as shown in Figure 3. A volume meshing option with a skewness of 0.67 was chosen to enable automatic meshing process. Mesh refinement was performed in the areas where a significant variation of airflow field occurred, precisely, close to the supply air diffusers, exhaust grilles, and surgical lamps.

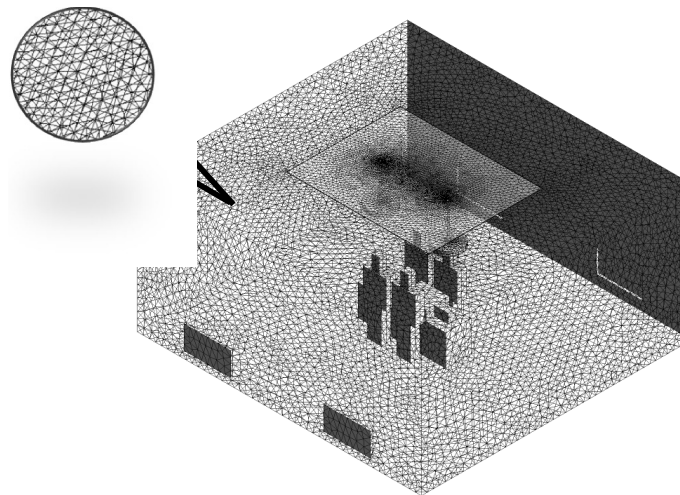


Fig. 3. Meshing of the operating room CFD model

2.3 Baseline Case Model Boundary Conditions

A baseline case model was developed to evaluate particles distribution in the vicinity of the operating table in the operating room when the effects of surgical lamps and medical staffs surface temperatures were not taken into account. The inlet air velocity of 0.32 m/s was prescribed at the

ceiling mounted air supply diffusers. Also, at such location, the air temperature and turbulence intensity were fixed at 19°C and 20%, respectively. A zero-gage pressure boundary condition was specified at each exhaust grille, which serves as the air outlets. The turbulence intensity of 10% and the air temperature of 21°C were also defined at the outlets. The prescriptions of the air temperature, inlet air velocity, and turbulent intensities were based on the work of Liu *et al.* [8]. All airflow boundary conditions were specified in the direction normal to the respective surfaces. The air flow inside the operating room was assumed as incompressible.

For the particle boundary conditions, an escape option was specified at the supply air diffusers and medical staff faces while a trap condition was set on the walls, patient and exhaust grilles. The trap boundary condition indicates that once a particle touches the solid surface, it remains, and the particle tracking process would stop. The escape boundary condition signifies that when the particle reaches the solid surface, the trajectory calculations end Liu *et al.* [8]. The particle size of 5 µm diameter or equivalent to 2 g/cm³ was considered as the released particles by each medical staff. The particles were assumed to be released from the face of the staffs, at a rate of 600 particles/minute which is equivalent to 1.31×10^{-12} kg/s. This value was chosen based on the work of Liu *et al.* [8]. The wall, medical staffs, patient, operating table, floor, and ceiling were specified as wall boundary conditions with a no-slip and stationary features. With this state, the fluid sticks to the wall, and its flow velocity gradually increases away from the walls. Table 2 summarizes the baseline case prescribed boundary conditions.

Table 2
 Baseline Case Boundary Conditions

Zone	Type	Boundary conditions
Air diffuser	Velocity inlet	Velocity magnitude: 0.32 m/s Temperature: 292 K Turbulent intensity: 20% DPM*: escape
Exhaust grille	Pressure outlet	Gauge pressure: 0 Pa Temperature: 294 K Turbulent intensity: 10% DPM*: escape
Surgical lamps	Wall	Wall condition: stationary Shear condition: no-slip DPM*: trap
Medical staff	Wall	Wall condition: stationary Shear condition: no-slip DPM*: escape
Walls	Wall	Wall condition: stationary Shear condition: no-slip Temperature: 294 K DPM*: trap

* Discrete phase model specification

2.4 Mesh Sensitivity Test

A mesh sensitivity test was carried out on the CFD model to ensure that the meshing has negligible effects on the results of the analysis through a grid independent test (GIT) analysis. Several sets of element numbers were tested under steady-state conditions, and the variation of airflow velocity at a selected location in the model versus a number of elements was plotted, as

shown in Figure 4. It can be seen that the airflow velocity was nearly unchanged when 1,174,520 elements were used to mesh the computational domain. Increasing the number of elements more than 1.2 million gives negligible effects on the airflow velocity of 0.238 m/s. Thus, 1,174,520 tetrahedral elements with non-structured meshing were considered adequate for the airflow and particle flow simulations and were adopted for all the proceeding simulations.

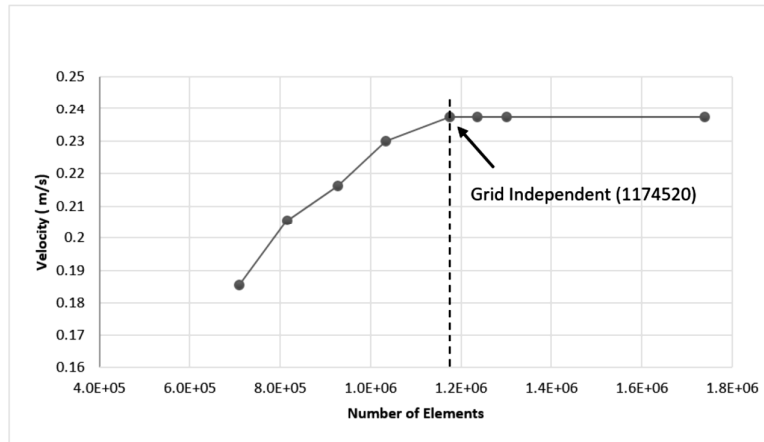


Fig. 4. Variation of airflow velocity with a number of elements

2.5 Selection of Airflow and Particle Flow Models

The governing equations that describe the fluid flow and particles concentration within an enclosure are all based on the conservation of mass, momentum, energy and species concentration. Several flow models are available in the CFD software to simulate the airflow inside a computational domain [6, 20]. However, according to Liu *et al.*, [8], the RNG k-epsilon model is adequate to give sufficiently reliable results for assessing a steady-state airflow and particles flow since it is capable of responding appropriately to the effects of rapid strain and streamline curvature. The governing equations that describe the fluid flow within an enclosure are all based on the conservation of mass, momentum and thermal energy [14]. The conservation of mass under steady state condition is given by Equation (1),

$$\frac{\partial}{\partial x}(u) + \frac{\partial}{\partial y}(v) + \frac{\partial}{\partial z}(w) = 0 \quad (1)$$

where u , v and w are the components of velocity in x , y and z directions, respectively. The momentum equations in x , y and z directions are expressed by Equations (2), (3) and (4), respectively,

$$\frac{\partial}{\partial t}(\rho u) + \frac{\partial}{\partial x}(\rho uu) + \frac{\partial}{\partial y}(\rho uv) + \frac{\partial}{\partial z}(\rho uw) = \rho g_x - \frac{\partial p}{\partial x} + R_x + \mu \left(\frac{\partial^2 u}{\partial x^2} + \frac{\partial^2 u}{\partial y^2} + \frac{\partial^2 u}{\partial z^2} \right) + \tau_x \quad (2)$$

$$\frac{\partial}{\partial t}(\rho v) + \frac{\partial}{\partial x}(\rho uv) + \frac{\partial}{\partial y}(\rho vv) + \frac{\partial}{\partial z}(\rho vw) = \rho g_y - \frac{\partial p}{\partial y} + R_y + \mu \left(\frac{\partial^2 v}{\partial x^2} + \frac{\partial^2 v}{\partial y^2} + \frac{\partial^2 v}{\partial z^2} \right) + \tau_y \quad (3)$$

$$\frac{\partial}{\partial t}(\rho w) + \frac{\partial}{\partial x}(\rho u w) + \frac{\partial}{\partial y}(\rho v w) + \frac{\partial}{\partial z}(\rho w w) = \rho g_z - \frac{\partial p}{\partial z} + R_z + \mu \left(\frac{\partial^2 w}{\partial x^2} + \frac{\partial^2 w}{\partial y^2} + \frac{\partial^2 w}{\partial z^2} \right) + \tau_z \quad (4)$$

where g is the gravity acceleration, μ is the effective viscosity, p is the pressure, R_i is the source term for distributed resistance (suffix i is x , y and z) and τ is the viscous stress. The energy equation is given in the following form:

$$\frac{\partial}{\partial t}(\rho C_p T_o) + \frac{\partial}{\partial x}(\rho u C_p T_o) + \frac{\partial}{\partial y}(\rho v C_p T_o) + \frac{\partial}{\partial z}(\rho w C_p T_o) = \frac{\partial}{\partial x} \left(K \frac{\partial T_o}{\partial x} \right) + \frac{\partial}{\partial y} \left(K \frac{\partial T_o}{\partial y} \right) + \frac{\partial}{\partial z} \left(K \frac{\partial T_o}{\partial z} \right) + W^v + E_k + Q_v + \Phi + \frac{\partial p}{\partial t} \quad (5)$$

where C_p is the specific heat, T_o is the total temperature, K is the thermal conductivity of air, W^v is the viscous work term, Q_v is the volumetric heat source, Φ is the viscous heat generation term, and E_k is the kinetic energy.

A semi-implicit method for pressure linked equations (SIMPLE) scheme was used in solving the pressure-velocity coupling calculation. The simulation was performed in a steady-state condition with the second-order upwind discretization scheme. The discretization scheme was selected as second-order upwind to reduce the effects of numerical diffusion on the solution as it would help improve the accuracy. Absolute residual value for all conservation equations was set to 1×10^{-4} except for the energy equation, where it was set to 1×10^{-6} . The convergence of the airflow velocity is shown in Figure 5.

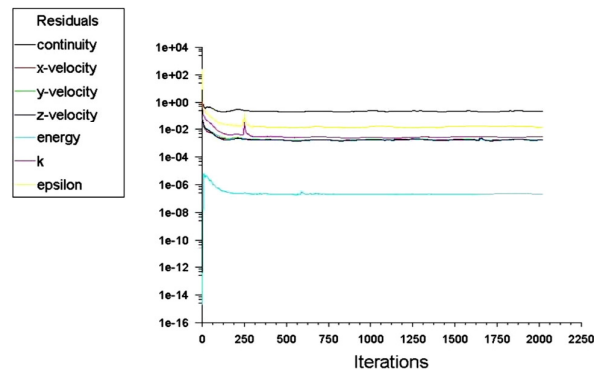


Fig. 5. Convergence of baseline case in steady-state

The discrete phase model (DPM) was used for simulating the particles flow in the OR CFD model. The DPM is based on the Euler-Lagrange approach, and it is appropriate for particles that occupy a volume fraction of less than 10% regardless of its mass fraction Rui *et al.* [15]. Many studies have shown that this model is reliable to be used in modelling particles movement [17-19]. The governing force balance equation for the discrete phase model (DPM) is given in Equation (6) below,

$$\frac{du_i^p}{dt} = F_D(u_i - u_i^p) + \frac{g_i(\rho_p - \rho)}{\rho_p} + \frac{F_i}{\rho_p} \quad (6)$$

where the first term on the right represents a drag force with a function of the relative velocity, the second term represents a gravity force, and the third term describes the Staffman lift and Brownian forces. Also, u_i is the fluid velocity, u_i^p is the particle velocity, ρ is the fluid density, ρ_p is the particle

density, the g_i is the gravitational acceleration and t is time. The Brownian and Staffman lift forces are used to model the movement of small particles having sizes ranging from $1 \mu\text{m}$ to $10 \mu\text{m}$.

2.6 Effects of Surgical Lamps and Staffs Surface Temperatures

A parametric analysis was conducted to evaluate the effects of surgical lamps and staffs surface temperatures on the particles distribution in the vicinity of the operating table. The same baseline CFD model of the OR was used for such analysis. However, each lamp and medical staff exposed surfaces were prescribed as wall boundary conditions with uniform temperatures of 45°C and 37°C , respectively. The exposed surface of the personnel was assumed to be at the body section as described in Table 1.

3. Results and Discussion

The results of the two different cases are compared to assess the effects of surgical lamps and medical staffs surface temperatures on the particles distribution in the vicinity of the operating table in steady-state conditions. Case (a) designates the baseline case, where the effects of surface temperatures of such bodies are neglected. Case (b) denotes the modified case, where the effects of surface temperatures of both groups are introduced into the analysis.

Figures 6 (a) and (b) show the airflow patterns inside the operating room in three-dimensional views for case (a) and case (b), respectively. As can be observed from Figure 6 (b), it was found that by introducing the surface temperatures of the surgical lamps and medical staffs in the analysis has developed more vortex currents in the vicinity of the operating table as compared to the baseline case in Figure 6 (a). A buoyance-driven airflow could cause such phenomena due to the difference in the air density between the hot surfaces and the adjacent air, which yields in the airflow deviation from the intended unidirectional airflow. Furthermore, since the lamps and medical staffs dwell within the operation zone and close to the operating table, further stimulate the unusual behaviour of the airflow in the vicinity of the operating table.

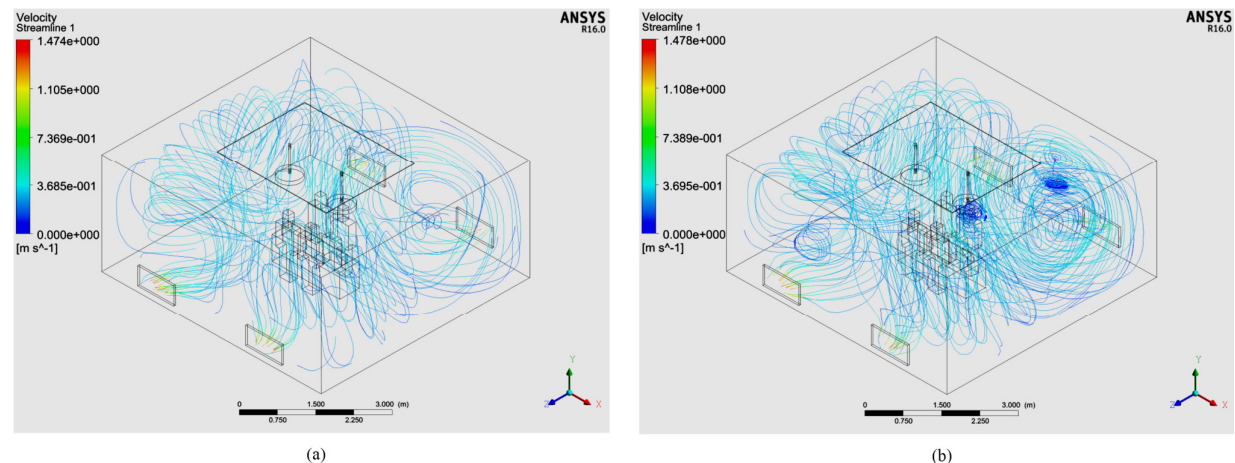


Fig. 6. Airflow streamline inside the operating room for (a) Case (a) – Baseline case; (b) Case (b) – Modified case

Figures 7 (a) & (b) show the airflow velocity contour in a vertical plane that passes through two medical staffs who are standing at the head-end of the operating table. It can be seen from the figures, when the personnel's body surface temperatures are considered in the analysis as shown in

Figure 7 (b), an outspread contour of the airflow velocity is growing significantly on both left and right sections of the surgical zone. However, when compared to the baseline case as illustrated in Figure 7 (a), such effects are lesser. It can also be observed from the two figures that the airflow velocity gradient on the left section of the surgical zone for case (b) is much higher than for case (a). The maximum magnitude of the airflow velocities in such area for both cases (a) and (b) are noticed to be approximately 0.34 m/s and 0.29 m/s, respectively, which is about 17% variation. On average, the magnitude difference of airflow velocity on the left sections of the operating zone between cases (a) and (b) is around 23%. In summary, the temperature difference of about 10°C between the staff body surfaces and the adjacent air could significantly influence the airflow velocity and interfere the unidirectional flow of the LAF diffuser. Similar conditions can be observed on the right side of both figures.

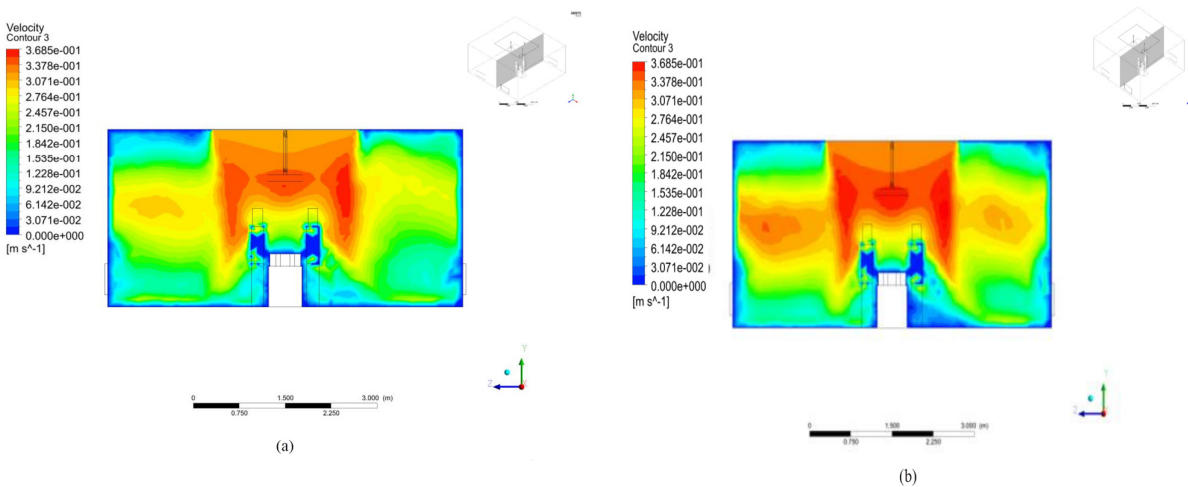


Fig. 7. Airflow velocity contour inside the operating room in a Y-Z plane for (a) Case (a) – Baseline case; (b) Case (b) – Modified case

Figures 8 (a) and (b) show the results of particle concentrations inside the operating room in a vertical plane that intersects through the medical lamps which are located directly below the inlet air diffuser and above the operating table for cases (a) and (b), respectively. It can be observed in both cases that a more significant number of particles appear to be on the floor of the adjacent area of the operating table head section. However, the thickness of the particles layer for case (b) is more prominent than for case (a), indicates that the effects of medical lamp temperatures on the particles amount in the vicinity of the operation zone are significant. It can also be seen from both figures that the highest particle concentration of $5.365 \times 10^{-4} \text{ mg/m}^3$ accumulates in the region close to the head section of the operating table. Also, for case (b) the highest particle concentration of the same magnitude occurs on the operating table. These findings indicate that the accumulation of particles on the operating table is affected by the temperature difference between the medical lamps and the next air causes buoyancy effects in the vicinity air. High accumulation of airborne particles in such area is unfavourable as this would increase the possibility of the particles to settle on the patient. In the actual surgical procedure, this would enhance the risk of the patient to be infected by the bacteria carried by the falling particles. In summary, when the surgical lamp and staff surface temperatures were prescribed at 45°C and 37°C, respectively, on average, the particle concentration in the vicinity of the operating table increases by 16%.

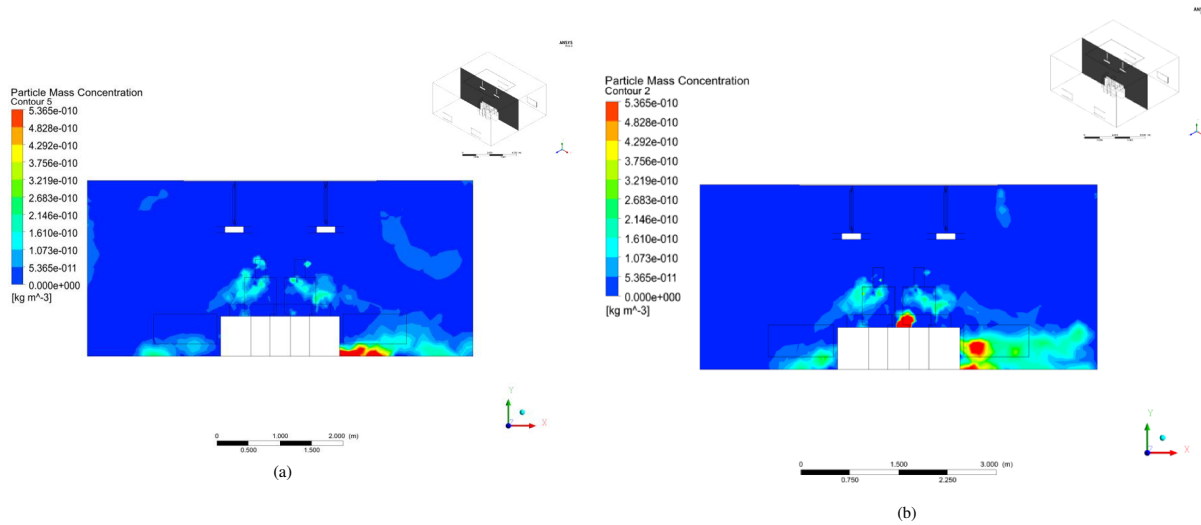


Fig. 8. Particles distribution inside the operating room in an X-Y plane for (a) Case (a) – Baseline case; (b) Case (b) – Modified case

Figures 9 (a) and (b) show the results of particle concentrations inside the operating room in a horizontal plane that passes through the medical staffs who are standing close to the operating table for cases (a) and (b), respectively. As the particles being released by the medical teams, the most significant number of particles can be observed in the vicinity of the staff bodies in both cases (a) and (b) as shown in Figure 9. It can be noticed from Figure 8 (b) that the particles merely dismissed from the personnel's body and moving toward the exhaust grille which is located at the left corner of the operating room. It can also be noticed from Figures 9 (a) and (b) that the number of particles nearby the medical staffs is more substantial for case (b) than the baseline case (a). A significant deviation of particles movement is undesirable as this would induce the particles to travel in arbitrary directions which in turn would sink onto the patient wound.

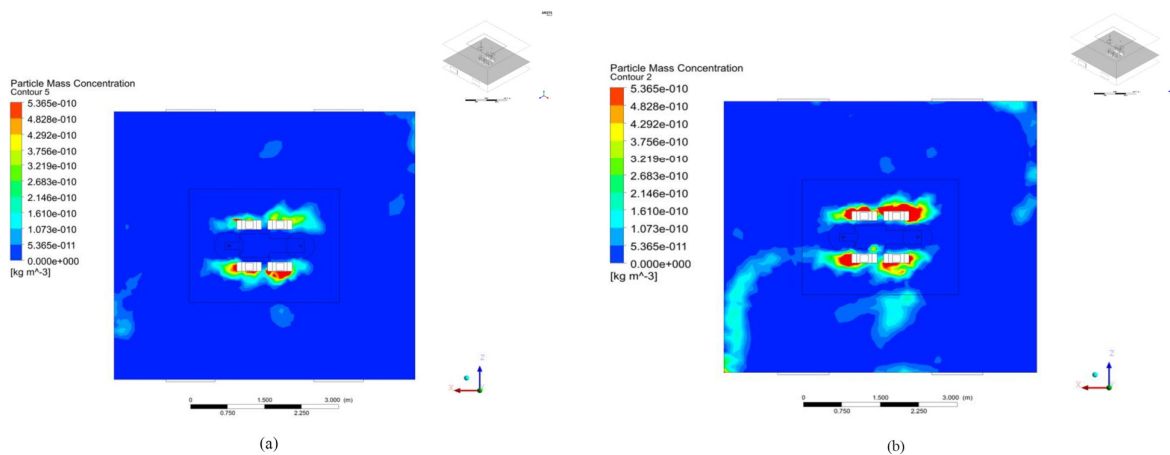


Fig. 9. Particles distribution inside the operating room in an X-Z plane for (a) Case (a) – Baseline case; (b) Case (b) – Modified case

4. Conclusion

A steady-state numerical analysis was carried out to investigate the effects of surface temperatures of surgical lamps and medical staffs on particles distribution inside an operating room equipped with a LAF ventilation system. A simplified model of the operating room was developed using Computational Fluid Dynamics (CFD) software. Particles with the size of 5 μm diameter were assumed to discharge from exposed faces of the surgical staff at a given mass flow rate. Results of the CFD simulations show that when the surgical lamp and staff surface temperatures were prescribed at 45°C and 37°C, respectively, on average, the particle concentration in the vicinity of the operating table increases by 16%. These findings indicate that the accumulation of particles on the operating table is affected by the surgical lamps and medical staffs' temperatures due to buoyance-driven force effects in the vicinity air.

Acknowledgement

The authors are grateful to the Universiti Teknologi Malaysia for providing the funding for this study, under the vote numbers of 14H64 and 20H44. Also, by the Ministry of Higher Education (MOHE) Malaysia under the Research University Grant. The grant was managed by the Research Management Centre, Universiti Teknologi Malaysia: FRGS Fund with the Vote No. 4F645.

References

- [1] Anderson, Deverick J., Kelly Podgorny, Sandra I. Berríos-Torres, Dale W. Bratzler, E. Patchen Dellinger, Linda Greene, Ann-Christine Nyquist et al. "Strategies to prevent surgical site infections in acute care hospitals: 2014 update." *Infection Control & Hospital Epidemiology* 35, no. S2 (2014): S66-S88.
- [2] Birgand, Gabriel, Gaëlle Toupet, Stephane Rukly, Gilles Antoniotti, Marie-Noëlle Deschamps, Didier Lepelletier, Carole Pornet et al. "Air contamination for predicting wound contamination in clean surgery: a large multicenter study." *American journal of infection control* 43, no. 5 (2015): 516-521.
- [3] Cristina, Maria Luisa, Anna Maria Spagnolo, Marina Sartini, Donatella Panatto, Roberto Gasparini, Paolo Orlando, Gianluca Ottria, and Fernanda Perdelli. "Can particulate air sampling predict microbial load in operating theatres for arthroplasty?." *PLoS One* 7, no. 12 (2012): e52809.
- [4] Chow, Tin-Tai, and Jinliang Wang. "Dynamic simulation on impact of surgeon bending movement on bacteria-carrying particles distribution in operating theatre." *Building and Environment* 57 (2012): 68-80.
- [5] Chow, Tin-Tai, and Xiao-Yu Yang. "Performance of ventilation system in a non-standard operating room." *Building and environment* 38, no. 12 (2003): 1401-1411.
- [6] Kamar, H.M., Nazri Kamsah, Kam, J.L. Indoor Air of a Double-Storey Residential House in Malaysia. *Journal of Advanced Research in Fluid Mechanics and Thermal Sciences* 31 (2017): 11-18
- [7] Karlatti, Suresh, and I. B. Havannavar. "A comparative prospective study of preoperative antibiotic prophylaxis in the prevention of surgical site infections." *International Surgery Journal* 3, no. 1 (2016): 141-145.
- [8] Liu, Junjie, Haidong Wang, and Wenyong Wen. "Numerical simulation on a horizontal airflow for airborne particles control in hospital operating room." *Building and Environment* 44, no. 11 (2009): 2284-2289.
- [9] Magill, Shelley S., Walter Hellinger, Jessica Cohen, Robyn Kay, Christine Bailey, Bonnie Boland, Darlene Carey et al. "Prevalence of healthcare-associated infections in acute care hospitals in Jacksonville, Florida." *Infection Control & Hospital Epidemiology* 33, no. 3 (2012): 283-291.
- [10] Mangram, Alicia J., Teresa C. Horan, Michele L. Pearson, Leah Christine Silver, and William R. Jarvis. "Guideline for prevention of surgical site infection, 1999." *American journal of infection control* 27, no. 2 (1999): 97-134.
- [11] Månsson, Emeli, Bengt Hellmark, Martin Sundqvist, and Bo Söderqvist. "Sequence types of Staphylococcus epidermidis associated with prosthetic joint infections are not present in the laminar airflow during prosthetic joint surgery." *Apmis* 123, no. 7 (2015): 589-595.
- [12] Memarzadeh, Farhad. "Reducing risks of surgery." *ASHRAE journal* 45, no. 2 (2003): 28.
- [13] Napoli, Christian, Vincenzo Marcotrigiano, and Maria Teresa Montagna. "Air sampling procedures to evaluate microbial contamination: a comparison between active and passive methods in operating theatres." *BMC Public Health* 12, no. 1 (2012): 594.

- [14] Prakash, D., and P. Ravikumar. "Analysis of thermal comfort and indoor air flow characteristics for a residential building room under generalized window opening position at the adjacent walls." *International Journal of Sustainable Built Environment* 4, no. 1 (2015): 42-57.
- [15] Rui, Zhang, Tu Guangbei, and Ling Jihong. "Study on biological contaminant control strategies under different ventilation models in hospital operating room." *Building and environment* 43, no. 5 (2008): 793-803.
- [16] Saadoun, Ismail, Ziad W. Jaradat, Ibraheem Ali Al Tayyar, Ziad El Nasser, and Qotaibah Ababneh. "Airborne methicillin-resistant Staphylococcus aureus in the indoor environment of King Abdullah University Hospital, Jordan." *Indoor and Built Environment* 24, no. 3 (2015): 315-323.
- [17] Sadrizadeh, Sasan, and Sture Holmberg. "Effect of a portable ultra-clean exponential airflow unit on the particle distribution in an operating room." *Particuology* 18 (2015): 170-178.
- [18] Sadrizadeh, Sasan, Sture Holmberg, and Ann Tammelin. "A numerical investigation of vertical and horizontal laminar airflow ventilation in an operating room." *Building and Environment* 82 (2014): 517-525.
- [19] Sadrizadeh, Sasan, Ann Tammelin, Peter Ekolind, and Sture Holmberg. "Influence of staff number and internal constellation on surgical site infection in an operating room." *Particuology* 13 (2014): 42-51.
- [20] Sapee, S. Computational Fluid Dynamics Study on Droplet Size of Kerosene Fuel. *Journal of Advanced Research in Fluid Mechanics and Thermal Sciences* 16 (2015): 1-14.
- [21] Sehulster, Lynne, Raymond YW Chinn, M. J. Arduino, J. Carpenter, R. Donlan, D. Ashford, R. Besser et al. "Guidelines for environmental infection control in health-care facilities." *Morbidity and mortality weekly report recommendations and reports RR* 52, no. 10 (2003).
- [22] Singh, Rajvir, Pooja Singla, and Uma Chaudhary. "Surgical site infections: Classification, risk factors, pathogenesis and preventive management." *Int. J. Pharm. Res. Health Sci* 2 (2014): 203-214.